JOURNAL OF MATERIALS SCIENCE 14 (1979) 2529–2536

Kinetics of crystallization of trans-1, 4-polyisoprene crystallized in thin films

C. K. L. DAVIES, ONG ENG LONG*
Department of Materials, Queen Mary College, Mile End Road, London E1 4NS, UK

The lamellar thickness and crystal growth rates of both high melting form and low melting form trans-1,4-polyisoprene crystals growing from the same melt in thin films, have been determined by transmission electron microscopy. Values of the fold surface energy (σ_e) have been determined and compare well with values for solution grown and bulk melt grown crystals. It is suggested that the crystals have a similar form in all three cases. The crystal growth rate data can be described by equations derived from secondary nucleation theory and the product of the surface energies ($\sigma_e \sigma_s$) is calculated. The value of the product is compared with recalculated values determined by using previously published optical growth rate data.

1. Introduction

A detailed electron microscope study of the morphology of trans-1,4-polyisoprene (TPI) crystallized in thin films has been reported previously [1]. Two crystalline forms of gutta percha (TPI) were observed and were defined as low melting temperature crystals (LMF) and high melting temperature crystals (HMF) on the basis of their equilibrium melting temperatures. Electron diffraction patterns from the LMF crystals were indexed using an orthorhombic unit cell [2, 3] and those from the HMF crystals using a monoclinic unit cell [3]. The growth faces for LMF TPI crystals were identified as {1 2 0}, and the probable growth faces for HMF TPI crystals as {1 1 0}.

The rates of spherulitic growth in TPI have been studied previously using optical microscopy by Henderson and Fisher [4] and Lovering [5, 6]. At the same crystallization temperature HMF spherulites grew faster as a result of higher degree of supercooling. The temperature dependence of the growth rates was discussed in terms of the secondary nucleation theory of polymer crystallization. The secondary nucleation constant was calculated and the product, $\sigma_s \sigma_e$ of the crystal fold surface energy (σ_e) and the crystal side surface energy (σ_s) determined. There is a considerable difference in the value of $\sigma_s \sigma_e$ calculated from the two studies largely as a result of very different equilibrium melting temperatures used. Estimates of σ_s and σ_e were made, but as no values of the lamellar crystal thicknesses were available an accurate value of σ_e and hence σ_s could not be determined. Subsequently the lamellar thickness of solution grown crystals was determined by X-ray diffraction studies of crystal mats [7, 8]. The X-ray long period was also determined for crystals grown from the melt [8]. From both these studies values of the fold surface energy (σ_e) were calculated.

The present study was initiated to test the existing theories of secondary nucleation [9, 10] on a system where two different crystal forms grow from the same melt. The thin film electron microscope method was adopted as this allows simultaneous measurements of lamellar thickness and crystal growth rate in the same specimen [11]. This allows $\sigma_s \sigma_e$ to be determined from the growth rate data and σ_e from variation of lamellar thickness with crystallization temperature, provided accurate values of the melting enthalpy (Δh_f) and the equilibrium melting temperatures

*Present address: Fundamental Chemistry and Physics Division, Rubber Research Institute of Malaysia, PO Box 150, Kuala Lumpur, W. Malaysia.

0022–2461/79/112529–08 $02.80/0

(T_m^0) are known. The study was also carried out to compare the growth rate parameters determined by optical microscopy with those determined from thin films in the electron microscope.

2. Experimental details

The TPI used in the investigation was a commercial grade of gutta percha* which was purified by solution precipitation [1]. The resulting polymer had an average viscosity molecular weight $\bar{M}_v$ of 385 000.

Samples of 2.5×10^{-5} m thickness were prepared for optical microscopy and heated to 90° C for half an hour to remove pre-existing nuclei by melting. The sample was then cooled rapidly to the desired crystallization temperature. All optical growth rate studies were carried out using a polarizing microscope equipped with a Mettler (FP2) heating stage. The temperature could be measured and automatically controlled to ± 0.1° C.

Crystal melting temperatures, following crystallization, were determined using differential scanning calorimetry at a heating rate of 10 K min^{-1}. The work was carried out using a Du Pont 900 Thermal Analyser.

Thin films of 100 nm thickness suitable for crystallization and for the subsequent electron microscopy study were prepared as reported previously [1], using the method devised by Andrews for thin films of cis-polyisoprene [12]. A 1% solution by mass in benzene of the purified polymer was heated to 65° C and small drops were placed on the surface of grease-free de-ionized water which was heated to 5° C above the required crystallization temperature. The solution spread, leaving a uniform thickness film after the benzene had evaporated. Some films were strained prior to crystallization by stretching on the water surface by means of a modified form of draftsman's dividers, similar to those described by Andrews [12]. When crystallization had occurred for a given time further crystallization was prevented by staining with osmium tetroxide vapour for about 45 sec. This also provides thickness contrast in the electron microscope. All films were examined in a JEM 7 electron microscope operated at 100 kV. HMF and LMF crystals were distinguished by either their respective electron diffraction patterns [1] or by the difference in melting temperatures [15] and at a later stage by the obvious difference in growth rates [13].

3. Results and discussion

3.1. Equilibrium melting temperatures

Following crystallization at a given temperature, the specimens were heated at 10 K min^{-1} and the melting temperature (T_m) determined. The melting temperature (T_m) as a function of the crystallization temperature (T_c) is shown for both crystal forms in Fig. 1. The plots are extrapolated linearly to the point where $T_m = T_c$ and the two equilibrium melting temperatures determined. This yields melting temperatures of 353 K and 362 K respectively for the LMF and HMF crystals.

Fisher and Henderson [4] used values of 337 K and 347 K in the analysis of the TPI optical microscope growth rate data. These values, determined by Mandelkern *et al.* [14], are certainly too low as they are the maximum melting temperatures observed rather than an extrapolated equilibrium melting temperature. Lovering and Wooden [15] determined the extrapolated equilibrium melting temperatures to be 351 ± 1.7 K and 360 ± 1.3 K. These values are very close to the present findings and are probably only slightly lower as a result of the slower heating rate of 1.35 K min^{-1} compared to the present rate of 10 K min^{-1}. These values were used by Lovering [5, 6] in the analysis of TPI optical growth rate data and will therefore be used to analyse all existing data and the present results. All three sets of values will be used on some of the data to compare the effect of T_m^0 on the predicted values of $\sigma_e\sigma_s$.

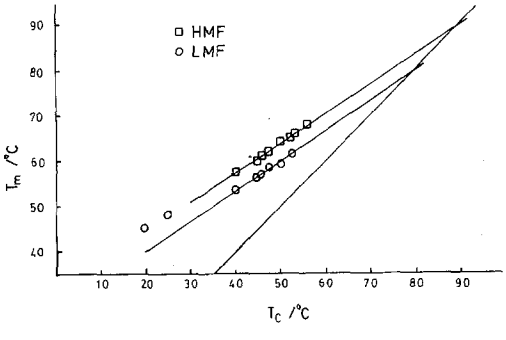

Figure 1 The measured melting temperature (T_m) as a function of the crystallization temperature (T_c).

*Penfold Golf Ltd., Birmingham, UK.

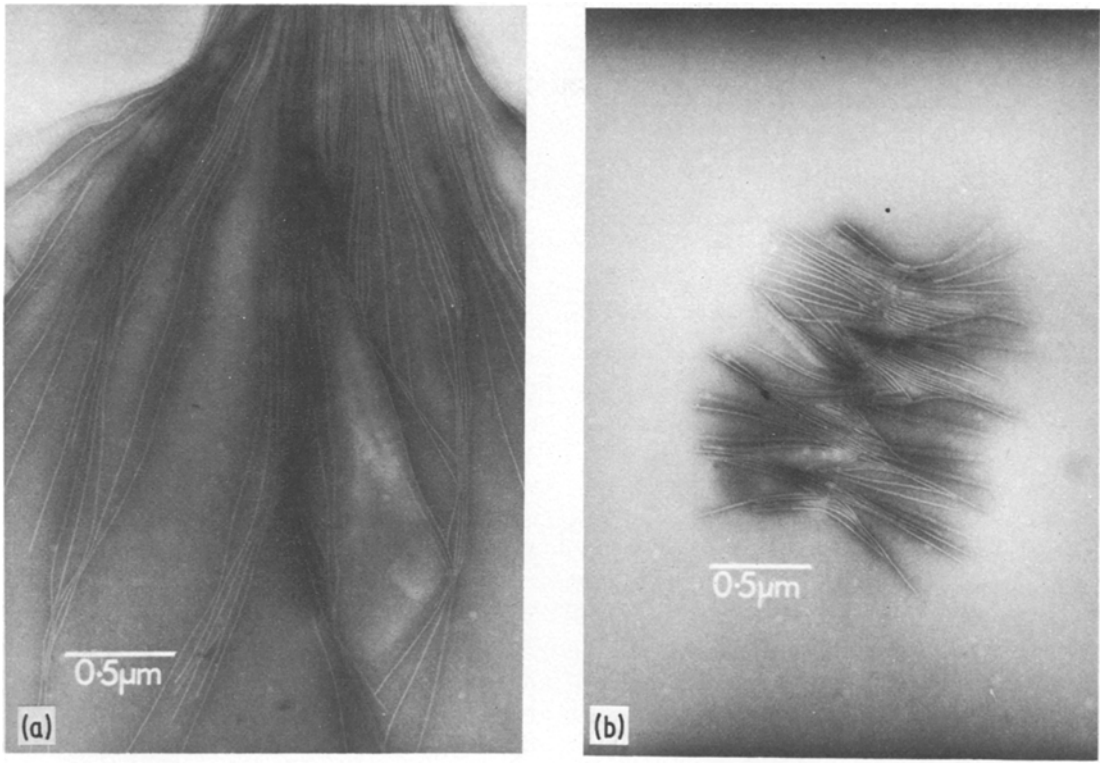

Figure 2 Electron micrographs showing lamellar crystals. (a) TPI crystallized for 1 h at 47° C showing LMF crystals. (b) TPI strained prior to crystallization for $\frac{1}{2}$ h at 50° C showing LMF crystals.

3.2. Lamellar thickness data

The lamellar thickness was determined by electron microscope observations of unstrained films or of films strained 50% prior to crystallization (Figs. 2a and b). For each crystallization temperature a large number of electron microscope photographic plates were taken of crystals with fold surfaces orientated near normal to the thin film surface. The minimum crystal thickness was determined from the plates, using a microdensitometer, and taken to be the observed lamellar thickness (l_{obs}) for that crystallization temperature. This thickness is plotted as a function of the crystallization temperature in the Fig. 3. Two lines are observed for HMF and LMF crystals respectively. In Fig. 4, l_{obs} is plotted as a function of the respective equilibrium melting temperatures (T_m^0) divided by the respective supercooling (ΔT). It can be seen that points for both HMF and LMF crystals and for both strained and unstrained films now lie on a single straight line.

The secondary nucleation theory [9, 10] predicts the initial crystal thickness to be of the form:

$$L = \frac{2\sigma_e T_m^0}{\Delta h_f \Delta T} + \delta l \qquad (1)$$

where Δh_f is the melting enthalpy and δl is small at low supercoolings. If the observed lamellar thickness (l_{obs}) is taken to be equal to L and Δh_f is known, a value of the fold surface energy (σ_e) can be determined. A reasonable estimate of Δh_f exists for HMF crystals but only a comparative value is known for LMF crystals [14]. These values are given as input data in Table II. The

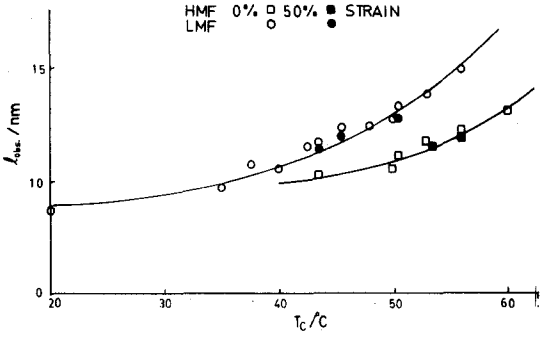

Figure 3 The observed lamellar thickness (l_{obs}) plotted as a function of the crystallization temperature (T_c).

TABLE I Values of σ_e for LMF and HMF trans-polyisoprene crystals

Source	Method	σ_e (J m^{-2})	
		HMF	LMF
Present work	Lamellar thickness from electron microscopy	60.1×10^{-3}	45.1×10^{-3}
A. Keller and E. Martuscelli [7, 8]	X-ray diffraction of stacks of solution grown crystals	72×10^{-3}	47×10^{-3}
E. Martuscelli [8]	From X-ray long period assuming crystallinity 40–50%		$41–51 \times 10^{-3}$

resulting calculated values of σ_e for HMF and LMF crystals are 60×10^{-3} J m^{-2} and 45×10^{-3} J m^{-2} respectively. These are compared with previous published values in Table I. It can be seen that the values are close to those for solution grown crystals determined by X-ray diffraction from single crystals mats [7, 8]. Martuscelli [8] determined the X-ray long period for LMF TPI crystallized in the bulk from the melt and assuming this to be the lamellar thickness calculated a value of σ_e of 102×10^{-3} J m^{-2}. However if the crystallinity were only 40 to 50% [13] and the structure consisted of crystals in a non-crystalline matrix this would yield a value for σ_e of between 41 and 51×10^{-3} J m^{-2}. This value is close to the values for both solution grown crystals [7, 8] and to the melt grown value determined by electron microscopy in thin films in the present work. The similarity in the values of the fold surface energy strongly suggests that the structure of the crystals is the same in all three cases. Furthermore, the single line obtained in Fig. 3 for both HMF and LMF crystals only occurs if $\sigma_e/\Delta h_f$ is equal for both crystal forms. This suggests that although the driving force for crystallization of HMF crystals is larger a greater penalty has to be "paid" in creating the fold surfaces as a result of the arrangements of molecules in the unit cell.

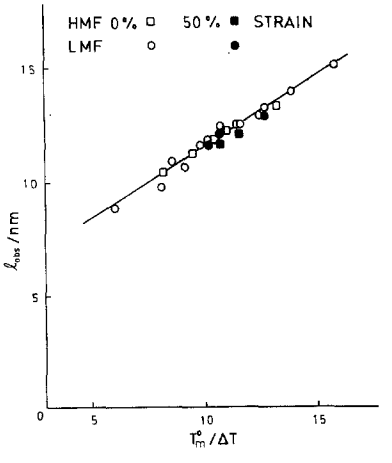

Figure 4 l_{obs} as a function of equilibrium melting temperature divided by the supercooling ($T_m^0/\Delta T$).

3.3. Growth rate data

The crystal and spherulite growth rates are determined in the thin films by transmission electron microscopy in the present work. This is carried out by determining the longest length of a crystal (strained films) and the largest diameter of a spherulite (unstrained films) after a given crystallization time. (Figs. 5a, and b and Fig. 2b). The measured growth rates (G) are shown as a function of the crystallization temperature in Fig. 6. It can be seen that over the temperature range studied HMF spherulites grow faster than LMF spherulites. However, if the growth rates are compared at the same supercooling, Fig. 7, the LMF spherulites have the faster growth rate.

The secondary nucleation theory represents the growth rate as a function of temperature by an equation of the form:

$$G = G_0 \exp\left(-\frac{\Delta G_\eta^*}{RT_c}\right) \exp\left(-\frac{K_g}{T_c \Delta T}\right)$$

where

$$\Delta G_\eta^* = C_1 T_c/(C_2 + T_c - T_g)$$

$$C_2 = 51.6\,\text{K}$$

$$T_g = 213\,\text{K}$$

$$K_g = 4b_0\sigma_s\sigma_e(T_m^0)^2/k\Delta h_f T_0$$

(for Regime I crystallization [10])

The exact form of the mobility term, the first exponential, is uncertain, but as only growth rate data at a temperatute above the growth rate

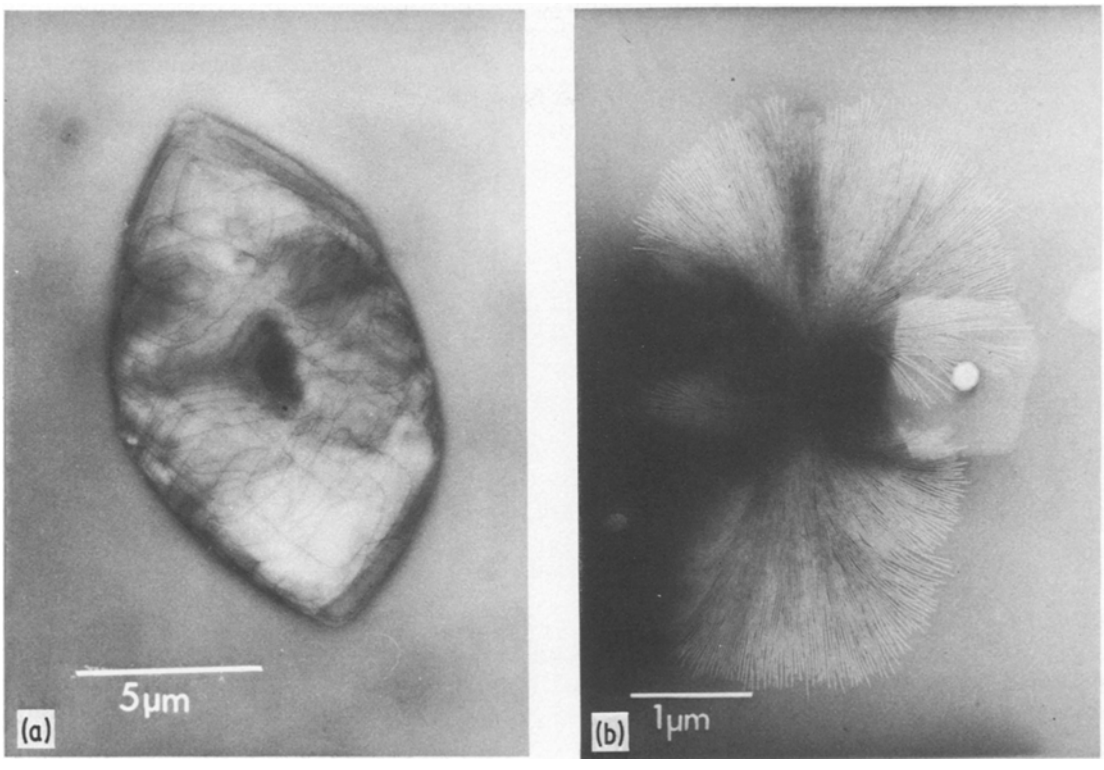

Figure 5 Electron micrographs showing growing spherulites. (a) TPI crystallized at 52° C for 1 h; HMF spherulite. (b) TPI crystallized at 45° C for $\frac{1}{2}$ h; LMF spherulite.

maximum is available for TPI it should not greatly affect the analysis. The activation energy ΔG_η^* is therefore approximated to the WLF expression [16]. The monomolecular layer thickness, b_0, is taken to be the interplanar spacing of the known growth planes [1]. All the input data is given in Table II. To test the validity of Equation 2 the growth rate data is plotted in the form

$$\log G + \Delta G_\eta^*/2.303RT_c \quad \text{versus} \quad \frac{10^2}{\Delta T}\left(\frac{T_m^0}{T_c}\right)^2$$

in Fig. 8. It can be seen that two straight lines are obtained for the two crystal forms suggesting that the secondary nucleation theory [9, 10] can be applied to the present data. The relationship between the HMF and LMF lines is unaffected by the form of the mobility term as both crystal forms grow from the same melt of the same polymer. Equation 2 can now be used to predict the whole of the growth rate temperature curve. This is shown in Fig. 9. The growth rate maxima would occur for both crystal forms at approxi-

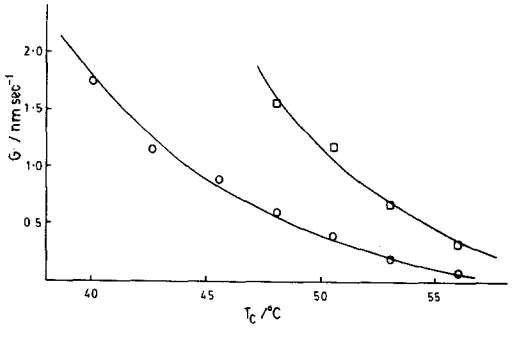

Figure 6 The crystal growth rate (G) as a function of the crystallization temperature (T_c).

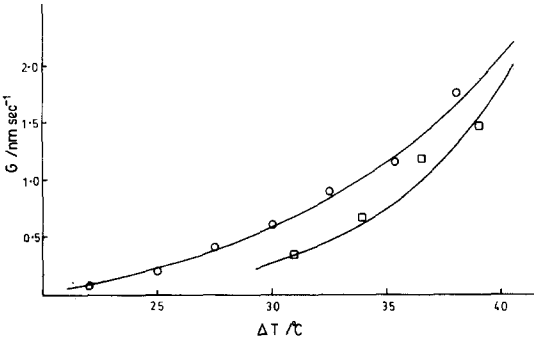

Figure 7 The crystal growth rate (G) as a function of the supercooling (ΔT).

TABLE II $\sigma_s\sigma_e$ from growth rate data for LMF and HMF trans-polyisoprene crystals

Input data	LMF	HMF
T_m^0 (K) [6]	351	360
T_g (K) [6]	213	213
Δh_f (J m^{-3}) [14]	0.75 × 1.98 × 10^8	1.98 × 10^8
b_0 (nm) (present work)	0.473	0.493
Source	$\sigma_c\sigma_s$ (J^2 m^{-4}	
	LMF	HMF
EM growth rates; present work	252 × 10^{-6}	490 × 10^{-6}
Optical [13]	–	640 × 10^{-6}
Optical [5, 6]	655 × 10^{-6}	–
Optical [4]; T_m^0 = 351 K	570 × 10^{-6}	839 × 10^{-6}
= 360 K	–	839 × 10^{-6}
Optical [4]; T_m^0 = 337 to 347 K	178 × 10^{-6}	382 × 10^{-6}
Optical [4]; T_m^0 = 353 to 362 K	645 × 10^{-6}	909 × 10^{-6}

mately 30° C. This fits with the observation that it is not possible to cool TPI to below room temperature without the specimen crystallizing totally. Furthermore it can be seen from Fig. 1 that the melting temperatures of specimens supposedly crystallized at temperatures below 30° C do not fit on the plot of T_m versus T_c. This is almost certainly because the specimens actually crystallized at a temperature around 30° C, the growth rate maximum. Fig. 9 shows that the growth rate of HMF crystals is always faster than that of LMF crystals at a given crystallization temperature. However if the predicted curves are plotted as a function of the supercooling they cross at a supercooling of approximately 40 K (Fig. 10). Thus although at low supercoolings LMF crystals grow faster, at larger supercoolings HMF crystals grow faster.

The slopes of the lines in Fig. 8 are given by $4b_0\sigma_s\sigma_e$. The products of the surface energies can therefore be calculated and values are given in Table II. It can be seen that the product for HMF crystals is much larger than that for LMF crystals. This is, of course, why the growth rate data for HMF and LMF crystals plotted as a function of supercooling, cross in Fig. 10. At low supercoolings the LMF crystals, while having the smaller driving force ($\Delta h_f \Delta T/T_m^0$), need less energy per area to

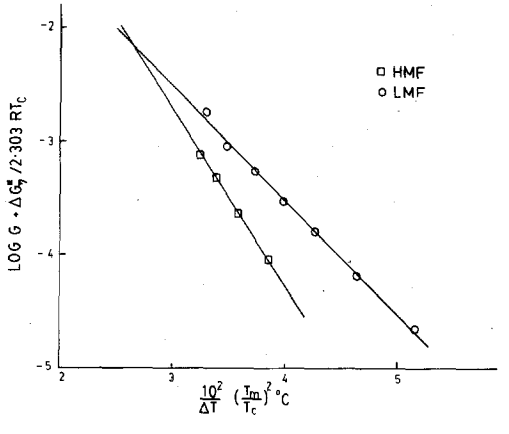

Figure 8 The growth rate plotted as a function of the crystallization temperature in the form

$$\log G + \Delta G^*_\eta/2.303RT_c \quad \text{versus} \quad \frac{10^2}{\Delta T}\left(\frac{T_m^0}{T_c}\right)^2 .$$

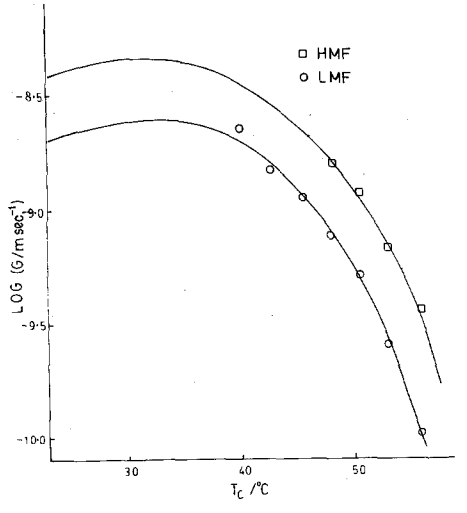

Figure 9 The predicted growth rate temperature curve.

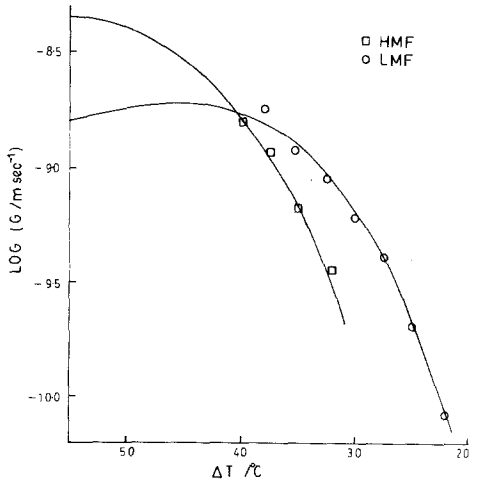

Figure 10 The predicted growth rate curve as a function of supercooling.

create surfaces ($\simeq \sigma_e\sigma_s$) and hence have the greater available driving force for growth. HMF crystals need a greater energy per area to create surfaces ($\simeq \sigma_e\sigma_s$) but the driving force increases much more rapidly with increasing supercooling as the surface energies are not very dependent on temperature. At large supercoolings the HMF crystals will therefore grow more rapidly than LMF crystals.

Table II also shows the values of the product $\sigma_s\sigma_e$ calculated from the various published optical growth rate data. The values have been calculated from the original growth rate data points, using the same input data as given in Table II in each case. It can be seen that in all cases the product $\sigma_s\sigma_e$ from the optical data is larger than that from the electron microscope data. These differences are only clear for the recalculated data using the same T_m^0 in all cases. At the bottom of Table II are shown values of $\sigma_e\sigma_s$ calculated from the Henderson and Fisher data [4], using the three available sets of values of T_m^0. It can be seen that the values of $\sigma_e\sigma_s$ for the present work are actually higher than the original Henderson and Fisher values [4], which were originally calculated using T_m^0 of 337 K and 347 K from the work of Mandelkern *et al.* [14]. In the case of TPI the optical growth rates are also, in general, faster than the electron microscope growth rates.

It is difficult to believe that the disparity in the $\sigma_s\sigma_e$ values is a consequence of the method of measurement, for in the case of isotactic polystyrene [17, 18] both methods give similar values and similar growth rates. There is considerable evidence to show that heating of polyisoprene in air at 90 to 100° C causes a reduction in molecular weight [19]. All the optical studies employ preheating of the specimens at this temperature in air while the electron microscope specimens were never heated to this temperature. If the optical microscope specimens have a lower molecular weight it would explain the faster growth rates as a result of increased mobility. This would however explain, only in part, the apparently high values of $\sigma_e\sigma_s$. The high values arising from the fact that difference in growth rates has been forced to appear in the $\sigma_e\sigma_s$ term as all other terms are held constant. The difference should have appeared in the mobility term through T_g. A high value of $\sigma_e\sigma_s$ implies a greater temperature dependence of the growth rate, not necessarily a faster growth rate. The value of σ_e from solution, bulk and thin films derived from the lamellar thickness data is very similar. The difference would therefore seem to be in σ_s. It is difficult to see why σ_s should be significantly affected by decreasing molecular weight and not σ_e. A possible explanation may be that the edge on [1] growing crystals in thin films touch the surfaces and hence have a lower σ_s due to surface nucleation. This is not an entirely convincing explanation as it could lead to flat on [1] crystals, which are completely contained within the film, growing at different rates from edge on crystals. This has never been observed.

3.4. Summary

The growth rates of both LMF and HMF trans-1,4-polyisoprene crystals, growing from the same melt in thin films, have been determined by transmission electron microscopy and the lamellar thickness of the crystals has been simultaneously measured. Values of the fold surface energy determined, agree very well with those determined for both solution grown crystals and for bulk crystallization from the melt. The growth rate data can be fitted to equations derived from secondary nucleation theory. The differences in growth rate of LMF and HMF crystals can be explained in terms of the differences of available driving force for the two crystal forms. Values of the product $\sigma_s\sigma_e$ have been calculated from the present growth rate data and compared with recalculated values of $\sigma_s\sigma_e$ from optical growth rate data. The higher values of $\sigma_s\sigma_e$ obtained from optical growth rates cannot be wholly explained

on the basis of oxidization degradation and the consequent reduction of molecular weight of optical microscope samples.

Acknowledgements

The authors would like to thank the Science Research Council for financial support for this work. One of the authors, Ong Eng Long, would like to thank the Malaysian Rubber Fund Board for the maintenance grant given during the period of his research. Thanks are also due to Dr D. A. Tod for carrying out the computer calculations and for helpful discussion. Finally, the authors would like to thank Professor E. H. Andrews for suggesting this work and for helpful discussion in the preparation of this paper.

References

1. C. K. L. DAVIES and ONG ENG LONG, *J. Mater. Sci.* **12** (1977) 2165.
2. C. W. BUNN, *Proc. Roy. Soc. Lond.* **A180** (1942) 40.
3. D. FISHER, *Proc. Phys. Soc. Lond.* **66** (1953) 7.
4. E. FISCHER and J. F. HENDERSON, *J. Polymer. Sci. A-2* **5** (1967) 377.
5. E. G. LOVERING, IUPAC Symposium on Macromolecules, Toronto (1968) Paper A6: 16.
6. *Idem, J. Polymer Sci. A-2* **8** (1970) 747.
7. A. KELLER and E. M. MARTUSCELLI, *Die Makro. Chemie* **151** (1972) 189.
8. E. MARTUSCELLI, *ibid.* **151** (1972) 159.
9. J. D. HOFFMAN and J. I. LAURITZEN Jr, *J. Res. Nat. Bur. Stand.* **65A** (1961) 297.
10. J. I. LAURITZEN Jr, and J. D. HOFFMAN, *J. Appl. Phys.* **44** (1973) 4340.
11. E. H. ANDREWS, P. J. OWEN and A. SINGH, *Proc. Roy. Soc.* **A324** (1971) 79.
12. E. H. ANDREWS, *ibid.* **A277** (1964) 562.
13. ONG ENG LONG, Ph.D. Thesis, University of London (1973).
14. L. MANDELKERN, F. A. QUINN and D. E. ROBERTS, *J. Amer. Chem. Soc.* **78** (1956) 926.
15. E. G. LOVERING and D. C. WOODEN, *J. Polymer Sci. A-2* **9** (1971) 175.
16. M. L. WILLIAMS, R. F. LANDEL and J. D. FERRY, *J. Amer. Chem. soc.* **77** (1955) 3701.
17. T. SUZUKI and A. J. KOVACS, *Polymer. J.* **1** (1970) 82.
18. B. C. EDWARDS and P. J. PHILLIPS, *Polymer* **15** (1974) 351.
19. J. L. BOLLAND, *Q. Rev.* **1** (1949) 3.

Received 3 November and accepted 23 November 1978.